International Journal of Applied Electromagnetics and Mechanics 46 (2014) 879–893
DOI 10.3233/JAE-140096
IOS Press

Semi-active vibration control of an aircraft panel using synchronized switch damping method

Hongli Ji[a,b,*], Jinhao Qiu[a], Hong Nie[a] and Li Cheng[b]
[a]*State Key Laboratory of Mechanics and Control of Mechanical Structures, Nanjing University of Aeronautics and Astronautics, Nanjing, Jiangsu, China*
[b]*Department of Mechanical Engineering, Consortium for Sound and Vibration Research, The Hong Kong Polytechnic University, Hung Hom, Kowloon, Hong Kong, China*

Abstract. With the rapid development of the aerospace industry, the control of aircraft structural vibration becomes increasingly important. Semi-active vibration control method based on synchronized switch damping have been attracted more attention due to its robustness compared with passive approaches and simplicity compared with active approaches. In this paper, three SSD semi-active control methods combined with a modal observer were applied to multimodal vibration suppression of an aircraft panel with stiffeners, and their effectiveness was verified by experimental results. A state observer was built based on the experimentally identified state-space model of the panel. Modal displacement of the panel was identified on line using the state observer and used in switch control of different piezoelectric actuators. Since the vibration characteristics of the panel with stiffeners was very complicated and its natural frequencies were distributed densely, use of the identified modal displacement as the reference signal for voltage switching in SSDI, SSDV and SSDNC improved the control effect for some specific modes and simplified the system. Good performances of vibration suppression were achieved in both single-mode control and multimodal control.

Keywords: Piezoelectric elements, synchronized switch damping, semi-active control, aircraft panel, state observer

1. Introduction

With the rapid development of the aerospace industry, the control of aircraft structural vibration becomes increasingly important. The vibration of aircraft structure not only deteriorates aircraft performance and leads to structural noise, but also causes fatigue failure of the structure. Due to the strict design specifications on weight and reliability of aircraft structures, it is necessary and urgent to develop high-performance vibration control systems with high reliability, lightweight, low power consumption. The passive approaches using damping materials can no longer meet the requirements, and vibration reduction based on piezoelectric elements has been proved to be a promising approach and mainstream of research. Piezoelectric materials are the most widely used functional materials and has the advantages

*Corresponding author: Hongli Ji, State Key Laboratory of Mechanics and Control of Mechanical Structures, Nanjing University of Aeronautics and Astronautics, Nanjing 210016, Jiangsu, China. Tel.: +86 25 848 911 23; Fax: +86 25 848 911 23; E-mail: jihongli@nuaa.edu.cn.

of high electromechanical coupling factor, small size, wide frequency band, et al., which are important for sensor or actuator applications in aerospace field [1].

Although significant progress has been achieved in the structural vibration control based on the piezoelectric elements in the past two decades, there are still many problems to be solved for real world applications. For example, active control methods give high control performance and robustness, but they need high-performance digital signal processing units and bulky amplifier. On the other hand, passive methods based on piezoelectric elements are easy to implement, but usually they are less robust. In order to overcome these disadvantages, several semi-active approaches have been proposed. Wang et al. studied a semi-active R-L shunting approach [2], in which an adaptive inductor tuning, a negative resistance and a coupling enhancement set-up lead to a system with damping ability. Davis et al. developed a tunable electrically shunted piezoceramic vibration absorber [3], in which a passive capacitive shunt circuit is used to electrically change the piezoceramic effective stiffness and then to tune the device response frequency. Clark, proposed a state-switched method [4], in which piezoelements are periodically held in the open-circuit state, then switched and held in the short-circuit state, synchronously with the structure motion.

Another type of semi-active control, which has been receiving much attention in recent years, is called pulse switching technique. It consists in a fast inversion of voltage on the piezoelement using a few basics electronics, which is synchronized with the mechanical vibration. In the methods proposed by Richard et al. the voltage on the piezoelectric element is switched at the strain extrema or displacement extrama of vibration [5]. These methods are called Synchronized Switch Damping (SSD) techniques [5–7]. On the other hand, in the method proposed by Onoda and Makihara the switch is controlled by an active control theory and it is called active control theory based switching technique here [8,9].

In the original SSD technique, the control performance mainly depends on the value of the voltage on piezoelectric element. To improve the control performance, an inductance can be connected to the shunt circuit to invert the voltage in the piezoelectric element. This method is called SSDI [6]. The inversion process boosts the voltage, thus increasing energy dissipation. The objective of all switch control algorithms is to maximize the energy dissipated in each cycle of vibration. To further improve the control performance, a method called SSDV (SSD based on voltage) has been proposed [7,10]. A new SSD method using negative capacitance (SSDNC) in the switching shunt circuits was proposed by the present author and her co-wokers [11–13]. Though the electric property of the whole circuit is capacitive, the voltage on the piezoelectric element can still be inverted efficiently in SSDNC method, which the synthesized negative capacitance is used to replace of inductor in SSDI control. The theoretical results show that the magnitude of the switched voltage on the piezoelectric element depends on the ratio of the inherent capacitance of the piezoelectric to the negative capacitance. Hence, the SSDNC method overcomes the disadvantage of SSDI that the magnitude of the switched voltage on piezoelectric elements depends on the voltage inversion coefficient, that is, the control performance is determined by quality factor of the inductor control.

Application of the SSD methods in multimodal vibration control has been of great interest and also of great challenge because defining optimal switching moment in a MDOF system is a very difficult issue. Several research works have been reported on application of the SSD techniques in multimodal vibration control. Corr and Clark [14] experimented with SSDI in the case of a multimodal vibration based on mode selection using digital filtering techniques. Harari used system identification method to estimate modal displacements and used them to control different modes in multi-mode control [15]. System identification method is superior to modal filtering method because no phase delay is induced in the estimated modal displacement. Goyumar and Badel [16] and Goyumar et al. [17] proposed a probabilistic approach and a statistical analysis dedicated to the SSD technique and achieved good control

performance. This control consists of defining optimal moments for the switching sequence in order to maximize the vibration damping and the energy dissipated in the switching device. Ji et al. proposed a displacement threshold technique and an energy based technique for switch control in SSDI and SSDV for their application in multimodal vibration control [18,19].

The techniques of SSD method for multimodal vibration control introduced above can be divided into two categories. The techniques in the first category use filter to select modes and the voltage is switched at the displacement extrema of the selected mode. Those in the second category use some algorithms to find the optimal switching moment in the resultant displacement of multimode vibration to maximize the converted energy. Although the techniques in the second category are effective for simple system with two or three modes, the algorithms to find the optimal switching moment may become very complicated when the number of modes increases. Hence for a complex system with many modes, multi-channel implementation of the techniques in the first category may be simpler because of the low cost of the SSD system.

In this study, an experimental platform of SSD method for vibration control of thin-wall aircraft structure was built. The effectiveness of SSD method in multimodal control was verified by experiment. The proposed new SSD semi-active control methods were applied to vibration suppression of an aircraft panel with stiffeners, and their effectiveness was verified by experimental results. Modal displacements of the panel were identified on line using the state observer and used in switch control of different piezoelectric actuators. Since the vibration characteristics of the panel was very complicated and its natural frequencies were distributed densely, use of the identified modal displacement as the reference signal for voltage switching in SSDI, SSDV and SSDNC improved the control effect for some specific modes and simplified the system. Good performances of vibration suppression were achieved in both single-mode control and multi-mode control.

2. Principle of ssd methods

2.1. Electromechanical model of a vibration system

As introduced above, modal displacements are necessary for voltage switching of piezoelectric actuators. Although the sensor signal contains the information of all the modal displacements to be controlled, they are mixed together. Hence, it is necessary to separate them using an observer. In order to identify the modal displacements, the state-space model of structure is necessary. The state-space model can be derived analytically, numerically or experimentally. In this study, the parameters of the state-space model were identified experimentally. The procedure is discussed in this section.

Figure 1 shows a generic structure with integrated piezoelectric patches (only one patch is shown in the figure). The vibration displacement $w(x,t)$ at any point of the structure, $\mathbf{x}$, can be written as the summation of the product of the modal coordinates and the eigenmode functions as follows:

$$w(x,t) = \sum_{i=1}^{n} \phi_i(x) u_i(t), \tag{1}$$

where $\phi_i(x)$ is the modal shape of the ith natural mode and $u_i(t)$ is its modal coordinate.

If it is assumed that the modal coordinates have been normalized with respect to modal mass, then the equation of motion in modal space after neglecting the high-order modes can be expressed in the following forms [15,19]:

$$\ddot{\mathbf{u}} + 2[\zeta_i \omega_i]\dot{\mathbf{u}} + [\omega_i^2]\mathbf{u} = -\mathbf{A}_1\mathbf{V}_1 - \mathbf{A}_2\mathbf{V}_2 + \mathbf{F}_e \tag{2}$$

where $\mathbf{u}$ is the vector of modal coordinates with length n, ω_i is the natural angular frequency of the ith natural mode when all the piezoelectric patches are in short-circuit state, ζ_i is the modal damping, $\mathbf{A}_1$ is the voltage coefficient matrix of piezoelectric patches used as actuators, and $\mathbf{A}_2$ is the voltage coefficient matrix of piezoelectric patches used as sensors. $\mathbf{V}_1$ and $\mathbf{V}_2$, having the dimension of k_1 and k_2 ($k_1 + k_2 = m$, the total number of piezoelectric patches), are the vectors of actuator voltages and sensor voltages, respectively. They are defined as follows:

$$\mathbf{A} = [\mathbf{A}_1|\mathbf{A}_2] = \begin{bmatrix} \alpha_{11} & \alpha_{12} & \cdots & \alpha_{1m} \\ \vdots & \vdots & & \vdots \\ \alpha_{n1} & \alpha_{n2} & \cdots & \alpha_{nm} \end{bmatrix}, \quad \mathbf{u} = \begin{Bmatrix} u_1 \\ \vdots \\ u_n \end{Bmatrix}, \quad \mathbf{F}_e = \begin{Bmatrix} F_{e1} \\ \vdots \\ F_{en} \end{Bmatrix},$$
$$[2\zeta_i\omega_i] = \begin{bmatrix} 2\zeta_1\omega_1 & \cdots & 0 \\ \vdots & \ddots & \vdots \\ 0 & \cdots & 2\zeta_N\omega_N \end{bmatrix}, \quad [\omega_i^2] = \begin{bmatrix} \omega_1^2 & \cdots & 0 \\ \vdots & \ddots & \vdots \\ 0 & \cdots & \omega_N^2 \end{bmatrix}, \tag{3}$$

The electrical equations of the piezoelectric patches can be expressed as

$$\begin{bmatrix} \mathbf{A}_1^T \\ \hline \mathbf{A}_2^T \end{bmatrix} \mathbf{u} - \left[\begin{array}{c|c} \mathbf{C}_{p1} & 0 \\ \hline 0 & \mathbf{C}_{p2} \end{array}\right] \begin{bmatrix} \mathbf{V}_1 \\ \hline \mathbf{V}_2 \end{bmatrix} = \begin{bmatrix} \mathbf{Q}_1 \\ \hline \mathbf{Q}_2 \end{bmatrix} \tag{4}$$

$\mathbf{C}_{p1}$ and $\mathbf{C}_{p2}$ are the diagonal matrix of inherent capacitance of the piezoelectric patches used as actuators and sensors, respectively, and $\mathbf{Q}_1$ and $\mathbf{Q}_2$ are the vector of electric charges on the piezoelectric actuators and sensors, respectively. They are defined as follows:

$$\mathbf{C}_p = \left[\begin{array}{c|c} \mathbf{C}_{p1} & \mathbf{0} \\ \hline \mathbf{0} & \mathbf{C}_{p2} \end{array}\right] = \left[\begin{array}{ccc|ccc} C_{p1} & & & & & \\ & \ddots & & & 0 & \\ & & C_{pk_1} & & & \\ \hline & & & C_{pk_1+1} & & \\ & 0 & & & \ddots & \\ & & & & & C_{pm} \end{array}\right], \quad \mathbf{Q} = \begin{Bmatrix} Q_1 \\ \vdots \\ Q_{k_1} \end{Bmatrix}, \tag{5}$$

If the input impedance of the sensor interface circuits is larger enough, the sensors can be assumed to be the open-circuit state, that is, the charges on the piezoelectric sensors are zero. This leads to

$$\mathbf{A}_2^T\mathbf{u} - \mathbf{C}_{p2}\mathbf{V}_2 = 0. \tag{6}$$

Substition of Eq. (6) into Eq. (2) yields

$$\ddot{\mathbf{u}} + 2[\zeta_i\omega_i]\dot{\mathbf{u}} + \left([\omega_i^2] + \mathbf{A}_2\mathbf{C}_{p2}^{-1}\mathbf{A}_2^T\right) u = -\mathbf{A}_1\mathbf{V}_1 + \mathbf{F}_e \tag{7}$$

If we define the state vector,

$$\mathbf{X}(t) = \begin{Bmatrix} \mathbf{u} \\ \hline \dot{\mathbf{u}} \end{Bmatrix} \tag{8}$$

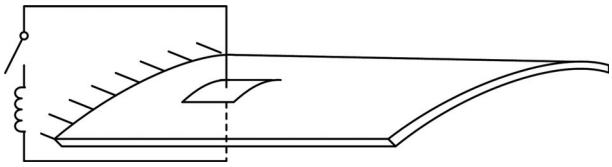

Fig. 1. A structure with bonded a piezoelectric element.

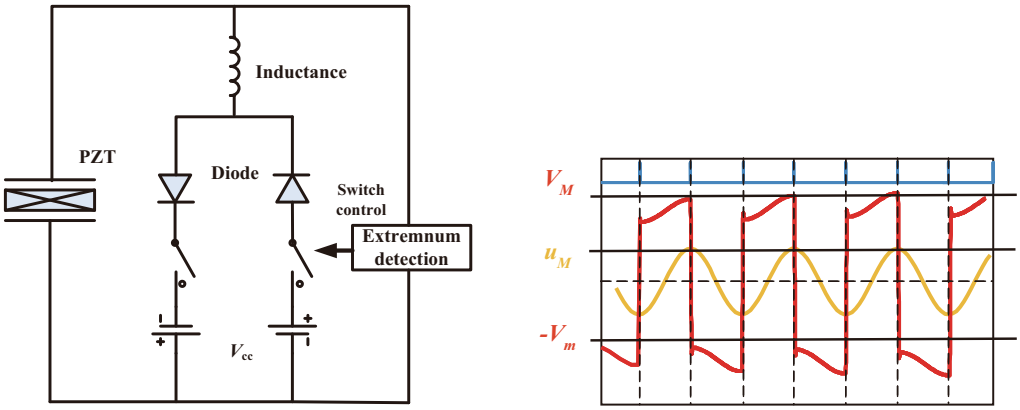

(a) The schematic of a SSDV circuit (b) The actuator voltage

Fig. 2. The principle of SSDV.

Then the system can be written in the following form:

$$\begin{aligned} \dot{\mathbf{X}}(t) &= \mathbf{A}_c\mathbf{X}(t) + \mathbf{B}_c\mathbf{u}_c(t) + \tilde{\mathbf{F}}_e(t) \\ \mathbf{y}_c &= \mathbf{C}_c\mathbf{X} \end{aligned} \tag{9}$$

where

$$\begin{aligned} &\mathbf{A}_c = \left[\begin{array}{c|c} 0 & I \\ \hline -\left([\omega_i^2] + A_2C_{p2}^{-1}A_2^T\right) & -[2\zeta_i\omega_i] \end{array}\right], \quad \mathbf{B}_c = \left[\begin{array}{c} 0 \\ \hline \mathbf{A}_1 \end{array}\right], \quad \tilde{\mathbf{F}}_e = \left[\begin{array}{c} 0 \\ \hline \mathbf{F}_e \end{array}\right] \\ &\mathbf{C}_c = \mathbf{C}_{p2}^{-1}\mathbf{A}_2^T, \quad \mathbf{u}_c = \mathbf{V}_1, \quad \mathbf{y}_c = \mathbf{V}_2 \end{aligned} \tag{10}$$

The term $\mathbf{A}_2\mathbf{C}_{p2}^{-1}\mathbf{A}_2^T$ is modification to the angular natural frequencies due to the electromechanical coupling effect of the piezoelectric patches in open-circuit state. For a structure considered in this study, the difference between the natural frequency in short-circuit state and that in the open-circuit state is very small, usually smaller than 0.1%. Hence, this term is neglected in the following discussion.

2.2. *Parameter identification*

The analytical expressions of the state-space model have been obtained in the previous section, but the values of the parameters need to be determined. Due to complexity of the structure, it is difficult to use the analytical for numerical method to obtain relatively accurate parameters in the state-space modal. Therefore, these parameters were identified by experimental methods in this study. There are standard

procedures to measure the modal frequency ω, modal damping ζ, and piezoelectric capacitance C_p by experiment, but there is no established method to identify the voltage coefficient matrix α_{ij}. The method of identification of α_{ij} used in this study is given below.

For convenience of analysis, it is assumed that the differences between the natural frequencies of different modes are large enough. It means that when a specific mode is excited by a harmonic force at its resonant frequency, the system can be considered as a SDOF system. That is, the vibration of this mode is dominant and the vibration of all other modes can be neglected.

Now it is assumed that the jth piezoelectric patch is used as an actuator and the other patches are used as sensors. A harmonic voltage, V_{ij}^a with a frequency of the ith modal is applied to the jth element, that is,

$$V_{ij}^a = \bar{V}_{ij}^a \cos \omega_i t, \tag{11}$$

where $\bar{V}_{ij}^a$ is the amplitude of V_{ij}^a.

According to the assumption above, the system is considered to be an SDOF system and according to Eq. (10), the equation of motion Eq. (7) is written as:

$$\ddot{u}_i + 2\zeta_i \omega_i \dot{u}_i + \omega_i^2 u_i = \alpha_{ij} V_{ij}^a, \tag{12}$$

The displacement response will be

$$u_i = u_{iM} \sin \omega_i t, \tag{13}$$

where

$$u_{iM} = \frac{\alpha_{ij} \bar{V}_{ij}^a}{2\zeta_i \omega_i^2}, \tag{14}$$

The sensor voltage on the kth piezoelectric element is:

$$V_{ik}^s = \frac{\alpha_{ik}}{C_{pk}} u_i. \tag{15}$$

According to the Eq. (15), the ratio of α_{ik} and α_{il}, the voltage coefficients of any two piezoelectric elements, can be expressed as:

$$\frac{\alpha_{ik}}{\alpha_{il}} = \frac{C_{pk}}{C_{pl}} \frac{V_{ik}^s}{V_{il}^s}. \tag{16}$$

If the values of the capacitances of the two elements are same, Eq. (16) can be simplified to:

$$\frac{\alpha_{ik}}{\alpha_{il}} = \frac{V_{ik}^s}{V_{il}^s} \quad (k \neq l). \tag{17}$$

According to Eq. (17), the ratio of voltage coefficients of two piezoelectric elements can easily be obtained by measuring their voltage outputs when the structure is excited at a specific mode.

Next the lth piezoelectric patch is used for excitation and the output voltage of the kth piezoelectric patch is measured. According to Eqs (14) and (15), there exist

$$u_{iM} = \frac{\alpha_{il} \bar{V}_{il}^a}{2\zeta_i \omega_i^2}, \text{ and } \bar{V}_{ik}^s = \frac{\alpha_{ik}}{C_{pk}} u_{iM}. \tag{18}$$

where $\bar{V}_{il}^a$ is the amplitude of voltage applied to the lth piezoelectric patch. From the Eq. (18), it is easy to obtain the following form:

$$\alpha_{ik}^2 = 2\zeta_i \omega_i^2 C_{pk} \frac{\alpha_{ik}}{\alpha_{il}} \frac{\bar{V}_{ik}^s}{\bar{V}_{il}^a}, \tag{19}$$

It shows that voltage coefficient α_{ik} can be calculated from Eq. (19) if the ratio of α_{ik}/α_{il} is known.

2.3. Review of the SSD methods

According to the previous work [20], the energy equation of the ith mode for a time window (0, T) can be expressed in the following form:

$$\int_0^T F_{ei}\dot{u}_i \mathrm{d}t = \int_0^T [2\zeta_i\omega_i]\dot{u}_i^2 \mathrm{d}t + \sum_{l=1}^{m}\int_0^T \alpha_{il}V_{il}\dot{u}_i \mathrm{d}t. \tag{20}$$

This equation exhibits that the provided energy is balanced by the energy dissipated on the mechanical damper and the converted energy, which corresponds to the part of mechanical energy which is converted into electrical energy. Maximizing this energy amounts to minimize the mechanical energy in the structure (kinetic + elastic). The purpose of the SSD method is to amplify the voltage on the piezoelectric element to improve the converted energy.

2.3.1. SSDI and SSDV methods

A typical switch circuit for SSDV method is shown in Fig. 2(a) and the corresponding actuator voltage is shown in Fig. 2(b). If there are no voltage sources in the circuit, it becomes the switch circuit of SSDI control. Between the actuator voltages V_M and V_m, there exist the following relationships:

$$V_m = \gamma V_M + (1+\gamma)V_{cc} \text{ and } V_M = V_m + 2\alpha u_M/C_p \tag{21}$$

where $\gamma \in [0, 1]$ is the voltage inversion coefficient, V_{cc} is the voltage source added in the circuit and u_M is the maximum amplitude of vibration displacement. The inversion coefficient γ is a function of the quality factor of the shunt circuit, Q_e:

$$\gamma = e^{-\pi/2Q_e} \tag{22}$$

From Eq. (21), the following switched voltage can be obtained:

$$V_{sw} = \frac{1}{2}(V_M + V_m) = \frac{1+\gamma}{1-\gamma}\left(\frac{\alpha}{C_p}u_M + V_{cc}\right). \tag{23}$$

The switched voltage can be effectively raised by increasing the output of the voltage source V_{cc}.

In steady-state control, the converted energy in a cycle of vibration can be expressed as:

$$\int_0^T \alpha V\dot{u}dt = 2\alpha u_M(V_m + V_M) = \left(\frac{4\alpha^2}{C_p}u_M^2 + 4\alpha u_M V_{cc}\right) \times \frac{1+\gamma}{1-\gamma}. \tag{24}$$

2.3.2. SSDNC method

The SSDNC system is the same as a SSDI system except that the inductance in SSDI is replaced by a negative capacitance. The schematic of the SSDNC system is shown in Fig. 3. The waveforms of the voltage on the piezoelectric element and the current in the circuit of SSDI are illustrated in Fig. 4(a). The SSDNC system is fundamentally first order because the electric circuit is purely capacitive [11]. No electrical oscillation occurs in the circuit. The waveforms of the voltage and current are illustrated in Fig. 4(b).

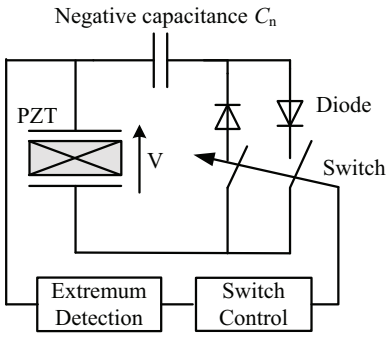

Fig. 3. The schematic of a SSDNC system.

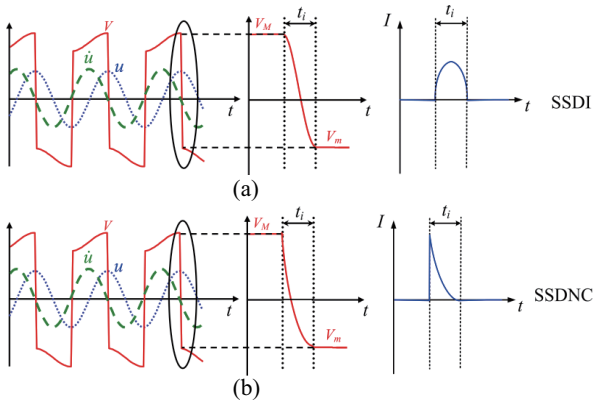

Fig. 4. The waveforms of the voltage on the piezoelectric actuator and the current in the circuit of SSDI and SSDNC.

In steady-state control, the voltage on the piezoelectric element and the converted energy in a cycle of vibration can be expressed as

$$V_m = -\frac{C_p}{C_n - C_p} \cdot \frac{\alpha}{C_p} u_M. \tag{25}$$

$$\int_0^T \alpha V \dot{u} dt = 2\alpha u_M (V_m + V_M) = \frac{C_n}{C_n - C_p} \frac{4\alpha^2}{C_p} u_M^2. \tag{26}$$

Equation (25) shows that the magnitude of the voltage after inversion is independent of the quality factor of the circuit, but dependent upon the capacitance ratio $C_p/(C_n - C_p)$. If the value of the negative capacitance, C_n, is slightly larger than the capacitance of the piezoelectric element, C_p, the amplification factor can be very large. This is the advantage of SSDNC.

Energy conversion and control voltage of SSDI and SSDNC with optimal switching frequency (switching at every displacement extrema) have been discussed in above. However, the voltage is not always switched at the optimal frequency in multi-modal control based on SSD techniques. Reference [12] shows that efficiency of energy conversion is reduced by about one half even if the switching frequency is slightly deviated from the optimal frequency, which is similar to the SSDI control system. However, the control performance of SSDNC is better than that of SSDI for most non-optimal switching frequencies. This is another advantage of SSDNC.

3. Modal observer and experimental system

3.1. Modal observer

In this study, a state-space observer was used to estimate the state vector, which contains the modal displacements as a sub-vector. The modal displacements are necessary in voltage switching of the piezoelectric actuators. The state-space model of the observer can be expressed in the following form:

$$\dot{\hat{\mathbf{X}}} = \mathbf{A}_c \hat{\mathbf{X}} + \mathbf{B}_c \mathbf{V}_a - K(\hat{\mathbf{V}}_s - \mathbf{V}_s) \tag{27}$$

Table 1
Parameters of the panel

Components	Parameters
Thickness of the aluminum	1 mm
Poisson ratio of the aluminum	0.33
Young's module of the aluminum	70 GPa
Density of the aluminum	2700 kg/m^3

Table 2
Physical properties and geometric data of the PZT element

Components	Parameters
Length	30 mm
Width	30 mm
Poisson ratio	0.345
Density	7400 kg/m^3
Thickness	0.2 mm
Piezoelectric constant d_{31}	-260×10^{-12} C/N
Capacitance C_p	61 nF

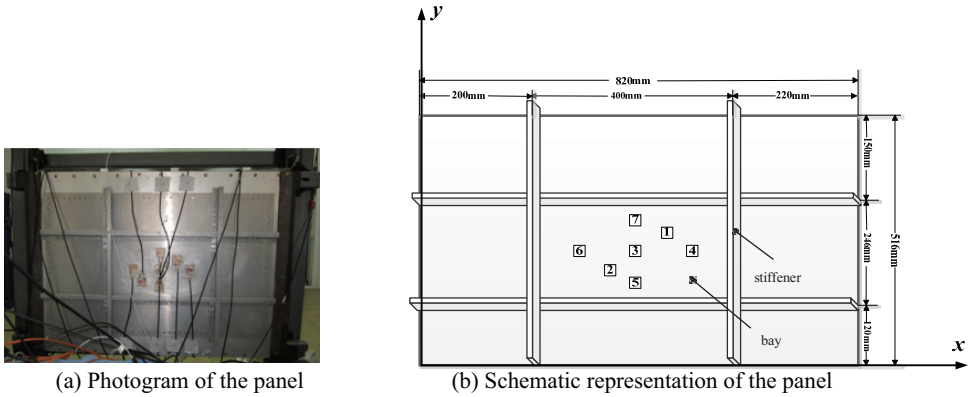

(a) Photogram of the panel (b) Schematic representation of the panel

Fig. 5. Experimental set-up.

where $\hat{\mathbf{X}}$ is the state variable of the observer, which is used to approximate the state variable the structure, $\mathbf{V}_a$ is the switched voltage on the piezoelectric actuator, $\mathbf{V}_s$ is the output of the piezoelectric sensor, and $\hat{\mathbf{V}}_s$ is the estimated sensor output from the observer. The matrix of gain K was designed using the Kalman filter approach [21]. Since the state variable of the state-space model of the structure is not available, the estimate state variable $\hat{\mathbf{X}}$, which include the modal displacement, was used for voltage switch.

3.2. Experimental set-up

The structure used in the experiment, shown in Fig. 5, was an aircraft panel. A laser Doppler vibrometer was used in experimental modal test of the aircraft panel and the layout of the piezoelectric elements was optimized based on the results of modal testing [22]. The parameters of the aircraft panel and piezoelectric elements are given in Tables 1 and 2. In this study, seven piezoelectric elements as shown in Fig. 5 were used. The layout of the piezoelectric elements is shown in Table 3. Piezoelectric patch 1 was used as the actuator for excitation of vibration of the panel. Piezoelectric patch 2 was used as a sensor to evaluate the performance of vibration control of the panel. Piezoelectric patches 3, 4 and 5 were used as actuator to control the vibration of the panel. According to the results of experimental modal test, the three piezoelectric patches were used for control of the three modes at 165.5 Hz, 232.2 Hz and 356.5 Hz, respectively, because they were most effective for the respective modes. Piezoelectric patch 6 was used in the observation of modal states.

The state-space observer shown in Eq. (27) was implemented in a DSP environment based on the dSPACE board DS1103. The block diagram of the whole system is shown in Fig. 6. The observed displacements $\hat{u}_1$, $\hat{u}_2$ and $\hat{u}_3$ were used as reference signals for voltage switching of piezoelectric patches 3,

Table 3
Layout of the PZT element

Number of piezoelectric elements	Layout of piezoelectric elements (x, y)
1	(450 mm, 270 mm)
2	(350 mm, 210 mm)
3	(400 mm, 243 mm)
4	(500 mm, 243 mm)
5	(400 mm, 180 mm)
6	(300 mm, 243 mm)
7	(400 mm, 300 mm)

Table 4
Parameters of the aircraft panel

	Mode 1	Mode 2	Mode 3
Modal frequency f_{i0}/Hz	165.5	232.3	356.5
Modal damping ξ_i	0.012	0.01	0.009

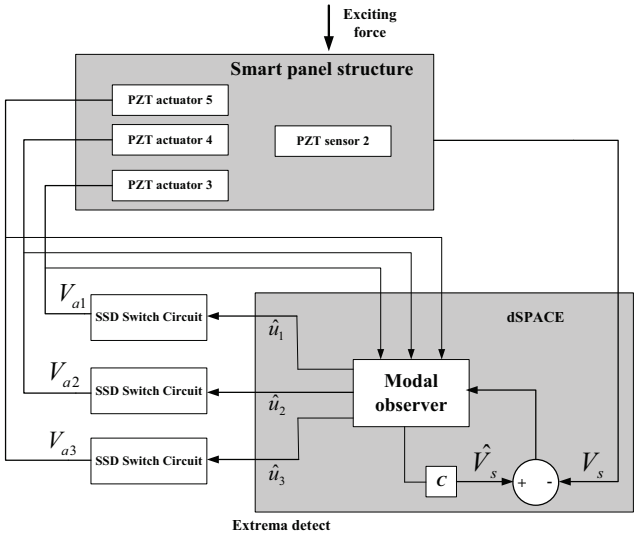

Fig. 6. SSD control system.

4 and 5. Switch signals were generated from the reference signals using extrema detect and used to control the switch circuits. The three SSD control approaches, SSDI, SSDV and SSDNC, were implemented on different switch circuits.

3.3. Parameter identification and observer performances

In this study, three selected modes with frequencies 165.5 Hz, 232.2 Hz and 356.5 Hz were controlled. The parameters of these modes were identified using experimental modal testing methods and are shown in Table 4. The voltage coefficients of the six piezoelectric elements coupled with the three modes were estimated using the procedure introduced in Section 2.3. The results are shown in Table 5.

To validate the performance of the observer, the uncontrolled response from piezoelectric patch 7 was measured and compared with the estimated responses. The results are presented in Fig. 7. Good agreement between spectrum of the measured response and that of the estimated response can be confirmed though there are differences in the peak values of the spectrum. Actually the peak values of the resonance are not very important for the generation of switch signal based on the principle of SSD control.

4. Experimental results and discussion

In order to evaluate the effectiveness of vibration suppression, the following performance index of vibration attenuation is defined,

$$A_i = 20\log\left(\frac{u_{iM(\text{with control})}}{u_{iM(\text{without control})}}\right) = 20\log\left(\frac{V_{siM(\text{with control})}}{V_{siM(\text{without control})}}\right). \tag{28}$$

A_i is negative if the vibration amplitude is reduced. The larger the absolute value of A_i, the better the control performance is.

Table 5
Voltage coefficient of the piezoelectric element

	$j=1$	$j=2$	$j=3$	$j=5$	$j=6$
α_{1j}	8.02E-03	4.09E-03	1.12E-02	3.79E-03	3.14E-03
α_{2j}	5.93E-03	7.33E-03	7.30E-03	5.93E-03	5.93E-03
α_{3j}	3.62E-02	1.35E-02	2.15E-02	4.81E-02	4.45E-02

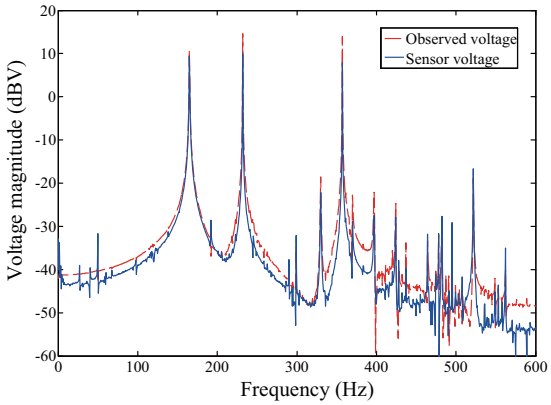

Fig. 7. Experimental non-controlled and identified model spectrum.

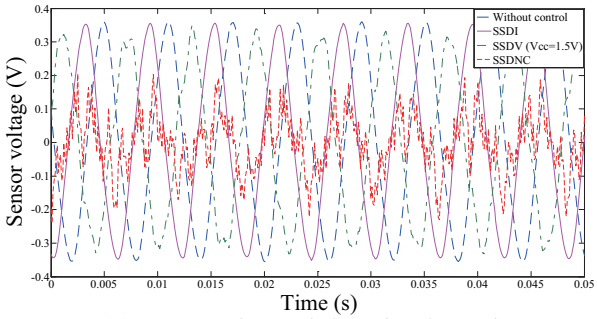

(a) Output voltage of piezoelectric patch 2

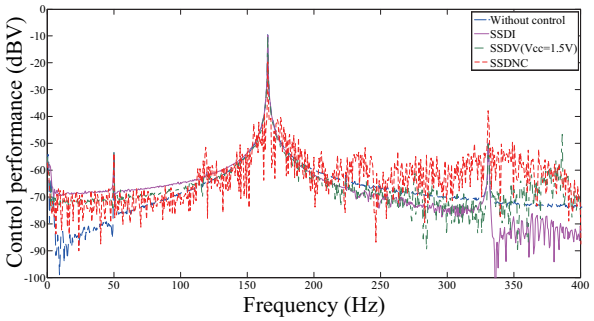

(b) Spectrum of the output voltage of piezoelectric patch 2

Fig. 8. Control performance using SSDI, SSDV, and SSDNC when excited at 165.5 Hz and using voltage of piezoelectric patch 6 as the reference for switch control.

4.1. Signal mode control

First control experiments were carried out when the aircraft panel was excited at the resonance frequency of a signal mode. Figure 8 shows the output voltages of piezoelectric patch 2 on the panel and their spectrum without control and with SSDI, SSDV and SSDNC controls when the panel was excited at the resonance frequency of 156.5 Hz and the output of piezoelectric patch 6 was used directly as the reference for switch control. The results show that the performance of the SSDI was very low and the amplitude of vibration control by SSDNC was smallest. The performance of SSDV was not much higher than that of SSDI. The main reason is that the components of high-frequency vibration were excited by the actuator voltage, which in turn generated extra switching points for the actuator voltage. As shown in the former study, the control performance of SSDV deteriorates considerably when switching frequency deviates from the optimal frequency [23].

The spectrum in Fig. 8(b) shows that components of high-frequency vibration were excited by the actuator voltage in SSDNC control. However, good control performance is still achieved for the vibration component at 156.5 Hz. There are two reasons for this result. The first is that the amplitude of actuator voltage in SSDNC control is determined by the ratio of the inherent capacitance of the piezoelectric actuator and the negative capacitance, as shown in Eq. (25). By choosing a suitable value of the negative capacitance, a large actuator voltage can be obtained. The second reason is that the control performance of SSDNC is kept in a relatively high level even if the switching frequency is deviated from the optimal frequency [12]. However, vibration level was obviously increased in the frequency range from 200 Hz to 400 Hz.

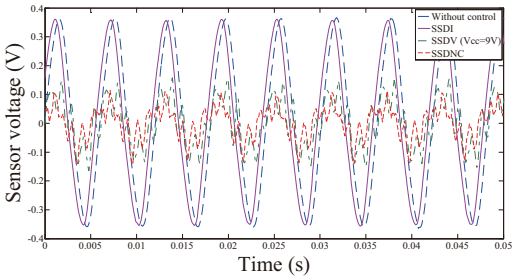

(a) Output voltage of piezoelectric patch 2

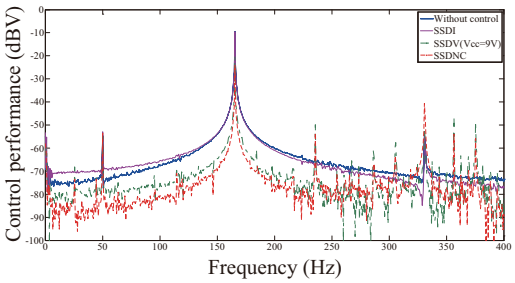

(b) Spectrum of the output voltage of piezoelectric patch 2

Fig. 9. Control performance using SSDI, SSDV, and SSDNC when excited at 165.5 Hz and using the estimated modal displacement as the reference for switch control.

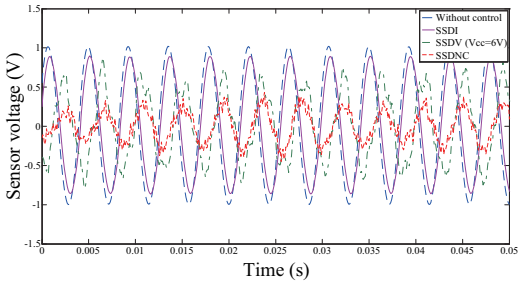

(a) Output voltage of piezoelectric patch 2

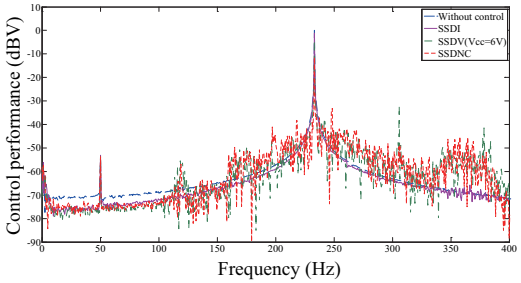

(b) Spectrum of the output voltage of piezoelectric patch 2

Fig. 10. Control performance using SSDI, SSDV, and SSDNC when excited at 232.3 Hz and using voltage of piezoelectric patch 6 as the reference for switch control.

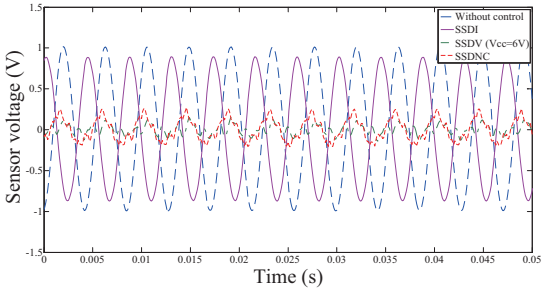

(a) Output voltage of piezoelectric patch 2

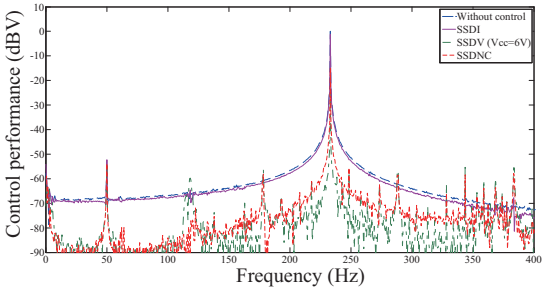

(b) Spectrum of the output voltage of piezoelectric patch 2

Fig. 11. Control performance using SSDI, SSDV, and SSDNC when excited at 232.3 Hz and using the estimated modal displacement as the reference for switch control.

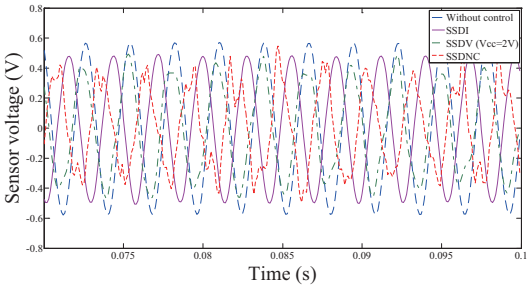

(a) Output voltage of piezoelectric patch 2

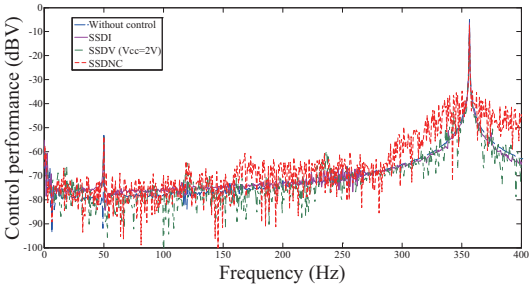

(b) Spectrum of the output voltage of piezoelectric patch 2

Fig. 12. Control performance using SSDI, SSDV, and SSDNC when excited at 356.5 Hz and using voltage of piezoelectric patch 6 as the reference for switch control.

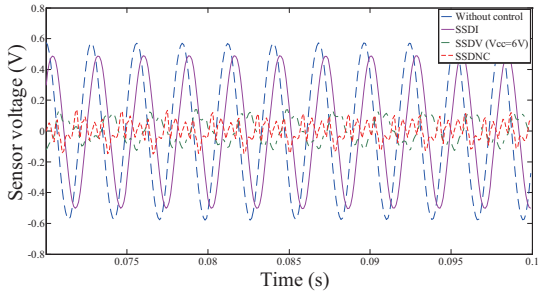

(a) Out put voltage of piezoelectric patch 2

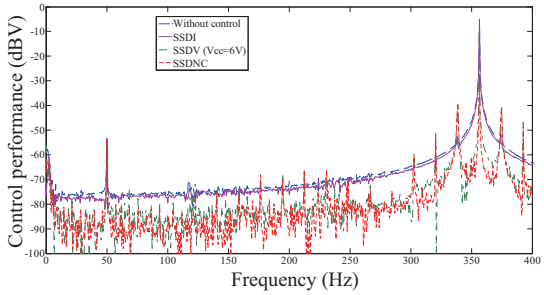

(b) Spectrum of the output voltage of piezoelectric patch 2

Fig. 13. Control performance using SSDI, SSDV, and SSDNC when excited at 356.5 Hz and using the estimated modal displacement as the reference for switch control.

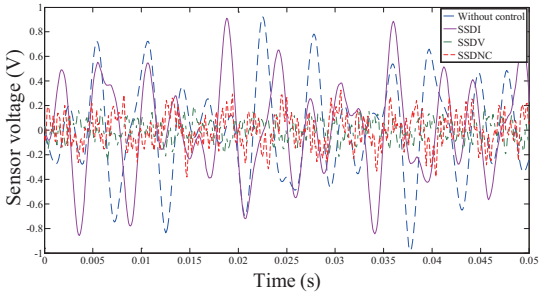

(a) Output voltage of piezoelectric patch 2

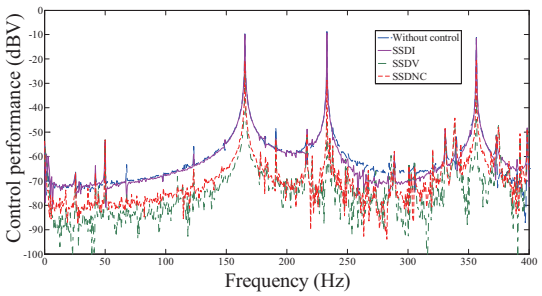

(b) Spectrum of sensor 2 voltage

Fig. 14. Control performance using SSDI, SSDV, and SSDNC when excited at three modes simultaneously and using the estimated modal displacement as the reference for switch control.

Figure 9 shows the same results as those in Fig. 8 when the estimated modal displacement $\hat{u}_1$ was used as the reference for switch control. Since the high frequency vibration was effectively filtered out by the observer, extra switch points were eliminated in switching signal. Hence the control performance of SSDV at the resonance frequency was significantly improved. The performance of SSDNV was also improved slightly. The high frequency vibration in the range from 200 Hz to 400 Hz was also suppressed except at several specific frequencies.

Figures 10 and 11 show the control results at the second resonance frequency of 232.3 Hz, using the original sensor output and the estimated modal displacement, respectively. Figures 12 and 13 show the control results at the second resonance frequency of 356.5 Hz, using the original sensor output and the estimated modal displacement, respectively. The results show that the uncontrolled modes were not obviously excited by the switched signal. These results experimentally verify the theoretical result that coupling of different modes are not induced by the switched voltage except at some specific frequency [24]. They also guarantee the feasibility of decoupled control of different modes using different actuators.

4.2. Multimodal control

In multimodal control, the three modes were excitely simultaneously at their resonant frequencies. The three modal displacements estimated by the observer were used as the reference signal for switch control of the three piezoelectric actuators to control the vibration of the three modes. Figure 14 shows the output voltages of piezoelectric patch 2 and their spectrum without control and with SSDI, SSDV and SSDNC controls when the panel was excited at the three resonance frequencies and the three modes

were controlled simultaneously by the three piezoelectric actuators. The results show that the SSDV method gives best performance among the three control methods used in this study. The reduction of vibration amplitude in multimodal vibration control is even better than that in single mode control for some modes. The results also confirm that the new method based on a state observer to estimate modal displacements is effective in multimodal control. Decoupled switch control of different piezoelectric patches considerably simplify the control system for the complicated structures, such as the aircraft panel with stiffener used in this study.

5. Conclution

Three SSD semi-active control methods, SSDI, SSDV and SSDNC, combined with a state observer have been applied to multimodal vibration suppression of an aircraft panel with stiffeners, and their effectiveness has been verified by experimental results. A new method for identification of voltage coefficients of different piezoelectric patches coupling with different vibration modes was proposed. The observer was built based on the experimentally identified state-space model of the panel. The modal displacements of the panel were identified on line using the state observer and used to control the voltage switching of three piezoelectric actuators independently. This scheme significantly simplify the control system and the switching algorithm. It also significantly improved the control performance of the SSDV and SSDNC methods, both in single mode control and multimodal control. The experimental results also show that SSDV yields the best control performance among the three methods.

Acknowledgments

This research is supported by the National Natural Science Foundation of China under Grant 51375228, Natural Science Foundation of Jiangsu Province under Grant BK20130791, the Fundamental Research Funds for the Central Universities under Grant NJ20140012, the NUAA Fundamental Research Funds under Grant NS2013008, and PAPD. It is also partially supported by the JSPS Core-to-Core Program, A. Advanced Research Networks, "International research core on smart layered materials and structures for energy saving".

References

[1] Y.S. Cheng, J.H. Qiu and H.J. Sun, A hybrid model of Prandtl-Ishlinskii operator and neural network for hystresis compensation in piezoelectric actuators, *International Journal of Applied Electromagnetics and Mechanics* **41** (2013), 335–347.

[2] K.W. Wang, J.S. Lai and W.K. Yu, Energy-based parametric control approach for structural vibration suppression via semi-active piezoelectric networks, *Transaction of ASME, Journal Vibration and Acoustics* **115** (1996), 505–509.

[3] C.L Davis, G.A. Lesieutre and J. Dosch, Tunable electrically shunted piezoceramic vibration absorber, *Proc SPIE, Smart Structures and Materials: Passive Damping and Isolation* (1997), 51–59.

[4] W.W. Clark, Semi-active vibration control with piezoelectric materials as variable stiffness actuators, *Proc 1000 AIAA/ ASME/ASCE/AHS/ASC Structures, Structural Dynamics, and Materials Conference and Exhibit* (1999), 2623–2629.

[5] C. Richard, D. Guyomar, D. Audigier and H. Bassaler, Enhanced semi passive damping using continuous switching of a piezoelectric device on an inductor, in: *Proceedings of SPIE International Symposium on Smart Structures and Materials: Damping and Isolation* **3989** (2000), 288–299.

[6] E. Lefeuvre, A. Badel, L. Petit, C. Richard and D. Guyomar, Semi-passive piezoelectric structural damping by synchronized switching on voltage sources, *J Intell Mater Syst Struct* **17** (2006), 653–660.

[7] A. Khodayari, A. Ahmadi and S. Mohammadi, On physical realization of the wireless semi active real time vibration control based on signal statistical behavior, *Sensors and Actuators A: Physical* **167** (2011), 102–109.
[8] J. Onoda, K. Makihara and K. Minesugi, Energy-recycling semi-active method for vibration suppression with piezoelectric transducers, *AIAA J* **41** (2003), 711–719.
[9] K. Makihara, K. Onoda and K. Minesugi, Low-energy-consumption hybrid vibration suppression based on an energy-recycling approach, *AIAA J* **43** (2005), 1706–1715.
[10] A. Badel, G. Sebald, D. Guyomar, M. Lallart, E. Lefeuvre, C. Richard and J.H. Qiu, Piezoelectric vibration control by synchronized switching on adaptive voltage sources: Towards wideband semi-active damping, *J Acoust Soc Am* **119** (2006), 2815–2825.
[11] H.L. Ji, J.H. Qiu, J. Cheng and D. Inman, Application of a negative capacitance circuit in synchronized switch damping techniques for vibration suppression, *Journal of Vibration and Acoustics, ASME* **133**(4) (2011), 041015.
[12] H.L. Ji, J.H. Qiu, P.Q. Xia and H. Nie, Energy conversion and performance of switched-voltage control based on negative capacitance with arbitrary switching frequency, *Smart Materials and Structures* **21**(12) (2012), 125010 (11pp).
[13] J. Cheng, H.L. Ji, J.H. Qiu and T. Takagi, Semi-active vibration suppression by a novel synchronized switch circuit with negative capacitance, *International Journal of Applied Electromagnetics and Mechanics* **37**(4) (2011), 291–308.
[14] L.R. Corr and L.R. Clark, A novel semi-active multi-modal vibration control law for a piezoceramic actuator, *Journal of Vibration and Acoustics, Transactions of the ASME* **125** (2003), 214–222.
[15] S. Harari, C. Richard and L. Gaudiller, New semi-active multi-modal vibration control using piezoceramic components, *J Intell Mater Syst Struct* **20** (2009), 1603–1613.
[16] D. Guyomar and A. Badel, Non-linear semi-passive multi-modal vibration damping: An efficient probabilistic approach, *J Sound Vib* **294** (2006), 249–268
[17] D. Guyomar, C. Richard and S. Mohammadi, Semi-passive random vibration control based on statistics, *Journal of Sound and Vibration* **307** (2007), 818–833.
[18] H.L. Ji, J.H. Qiu, A. Badel, Y.S. Chen and K.J. Zhu, Multimodal vibration control using a synchronized switch based on a displacement switching threshold, *Smart Materials and Structures* **18** (2009), 035016 (8pp).
[19] H.L. Ji, J.H. Qiu, K.J. Zhu and A. Badel, Two-mode vibration control using nonlinear synchronized switching damping based on the maximization of converted energy, *J Sound Vib* **329** (2010), 2751–2767.
[20] H.L. Ji, J.H. Qiu and K.J. Zhu, Vibration control of a composite beam using self-sensing semi-active approach, *Chinese Journal of Mechanical Engineering* **23**(5) (2010), 663–670.
[21] H. Kwakernaak and R. Sivan, Linear optimal control systems, New York: Wiley-Interscience, (1972), 220–222.
[22] M. Yuan, H.L. Ji, J.H. Qiu and T.B. Ma, Active control of sound transmission through a stiffened panel using a hybrid control strategy, *J Intell Mater Syst Struct* **23**(7) (2013), 791–803.
[23] H.L. Ji, J.H. Qiu, P.Q. Xia and I. Daniel, Analysis of energy conversion in switched-voltage control with arbitrary switching frequency, *Sensors and Actuators A: Physics* (174) (2012), 162–172.
[24] H.L. Ji, J.H. Qiu, P.Q. Xia and I. Daniel, Coupling analysis of energy conversion in multi-mode vibration structural control using synchronized switch damping method, *Smart Materials and Structures* **21**(1) (2012), 015013 (16pp).